Supporting Information

Elemental Anisotropic Growth and Atomic-Scale Structure of Shape-Controlled Octahedral Pt-Ni-Co Alloy Nanocatalysts

Rosa M. Arán-Ais[1], Fabio Dionigi[2], Thomas Merzdorf[2], Martin Gocyla[3], Marc Heggen[3], Rafal E. Dunin-Borkowski[3], Manuel Gliech[2], José Solla-Gullón, Enrique Herrero[1], Juan M. Feliu[1], Peter Strasser[2].

[1]*Instituto de Electroquímica, Universidad de Alicante, Apartado 99, 03080 Alicante, Spain.*

[2]*The Electrochemical Energy, Catalysis, and Materials Science Laboratory, Department of Chemistry, Chemical Engineering Division, Technical University Berlin, 10623 Berlin, Germany.*

[3]*Ernst Ruska-Centre for Microscopy and Spectroscopy with Electrons, Forschungszentrum Jülich GmbH, 52425 Jülich, Germany.*

Corresponding authors: pstrasser@tu-berlin.de; juan.feliu@ua.es

Materials and Methods

Chemicals. Platinum(II) acetylacetonate [$Pt(acac)_2$], nickel(II) acetylacetonate [$Ni(acac)_2$], cobalt(II) acetylacetonate [$Co(acac)_2$], potassium acetylacetonate [K(acac)] and anhydrous ethanol were purchased from Alfa Aesar. Nafion and N,N-dimethylformamide (DMF) were purchased from Sigma-Aldrich. All the chemicals were used as received without further purification.

Synthesis of octahedral PtNiCo/C catalysts.

One-step synthesis. 4 mM $Pt(acac)_2$, 10 mM $Ni(acac)_2$ and x mM $Co(acac)_2$ (x = 0, 2, 10, 20, 60 and 100) were dissolved in 50 mL DMF. The resulting homogeneous pink solution was inserted in a glass-lined stainless-steel autoclave (100 mL/100 bar Model I Roth). The sealed autoclave was heated from room temperature to 130 ºC, stirring during the first 30 min of the process. After 42 hours of reaction, octahedral $Pt_{30}Ni_{51}Co_{19}$ nanocrystals were obtained. The resulting solution was naturally cooled down to room temperature. A portion of the black product was kept and washed once with ethanol for electron microscopy characterization. The carbon support (Vulcan XC72R carbon) was added to the remaining solution, which was ultrasonicated for 30 min and aged overnight. Finally, the $Pt_{30}Ni_{51}Co_{19}$/C was washed 3 times with ethanol/water mixture (1:4) and twice with MilliQ water. The resulting electrocatalyst powder was obtained by freeze-drying.

The synthesis performed at 160 and 200 °C were carried out following the same procedure, using $Co(acac)_2$ concentrations of 0, 2, 6 and 10 mM.

Two-step synthesis. (A) Time optimization process: 4 mM $Pt(acac)_2$ and 10 mM $Co(acac)_2$ were dissolved in 50 mL DMF. The resulting homogeneous pinkish solution was inserted into a glass-lined stainless-steel autoclave. The sealed autoclave was heated from room temperature to 130 ºC, stirring during the first 30 min of the process. The temperature was kept for 42-x hours (time t_1). Once the solution was cooled down to room temperature, the autoclave was opened

and $Ni(acac)_2$ was added into the previous solution to achieve a final concentration of 10 mM. The temperature was raised back to 130 ºC and kept for x hours (time t_2). To study the Pt/M ratio and the NP's morphology, three time combinations were tested: 16 h/26 h, 24 h/18 h and 32 h/10 h. **(B) Control of Pt/M ratio:** In the first step of the synthesis, 4 mM $Pt(acac)_2$ and x mM $Co(acac)_2$ were dissolved in 50 mL DMF and kept at 130 ºC for 24 h. The second step consisted in the addition of x mM of $Ni(acac)_2$ to the solution, heating the mixture at 130 ºC for 18 h. The concentrations tested were x = 5, 10 and 15 mM. In the synthesis with the lowest content of non-noble metals precursors, 0.25 mmol of K(acac) was added in the first step of the synthesis. All samples were cooled down and supported on carbon as previously described.

Synthesis of octahedral PtNi/C and PtCo/C catalysts.

Octahedral PtNi NCs were obtained by the one-step synthesis described above: $Pt(acac)_2$ and $Ni(acac)_2$ were dissolved in 50 mL of pure DMF, achieving a final concentration of 4 and 10 mM, respectively. The precursor solution was transferred into a glass-lined stainless-steel autoclave. The system was heated from room temperature to 130 °C, keeping at this temperature for 42 h. The carbon support is added to the resulting cooled solution and the sample was treated as mentioned above.

Octahedral PtCo NCs were synthesized by replacing $Ni(acac)_2$ with $Co(acac)_2$ at the same concentrations while keeping all other conditions constant.

Materials characterization

Transmission electron microscopy (TEM) images were taken using a JEOL JEM-1400 Plus working at 120 kV. For the estimation of the mean particle size and size distribution of each sample, more than 200 particles from different parts of the grid were accounted.

Scanning transmission electron microscopy (STEM) was performed using an FEI Titan 80-200 ("ChemiSTEM") electron microscope, equipped with a Cs-probe corrector (CEOS GmbH) and high-angle annular dark field (HAADF) detector operated at 200 kV. In order to achieve "Z-

Contrast" conditions a probe semi-angle of 25 mrad and an inner collection semi-angle of the detector of 88 mrad were used. Compositional maps were obtained with Energy-dispersive X-ray spectroscopy (EDX) using four symmetric large-solid-angle silicon drift detectors. For EDX measurement an FEI double-tilt holder was used and the TEM specimen was untilted. The software ESPRIT (Bruker Company, Berlin, Germany) was applied for EDX analysis using the Pt L, Ni K and Co K peaks.

The atomic composition of the different catalysts was determined by inductively coupled plasma mass spectroscopy (ICP-MS) using a 715-ES-ICP analysis system (Varian). The samples were prepared by dissolving the catalysts powders in a mixture of H_2SO_4, HNO_3 and HCl (1:1:3). The solutions were heated from room temperature to 180 °C in 10 min using a Microwave Discover SP-D (CEM corporation), keeping at this temperature during 20 min. Finally, the cooled solutions were diluted with MilliQ water, filtered and taken to a known volume.

X-ray powder diffraction (XRD) patterns were collected using a D8 Advance-Diffractormeter (Bruker) equipped with a Lynx Eye Detector and KFL Cu 2K X-ray tube.

2D and 3D models were represented by using Vesta program [1].

Electrochemical measurements.

A three-electrode cell was used to perform the electrochemical measurements, with a platinum wire as a counter electrode and a reversible hydrogen electrode (RHE), connected to the cell through a Luggin capillary, as reference electrode (Hydroflex, Gaskatel). The working electrode was prepared by dropping a 10 μL aliquot of the catalyst ink onto a glassy-carbon Rotating Disk Electrode (RDE) (diammeter: 5 mm, area: 0.196 cm^2) from Pine Instruments. This ink was prepared by dispersing the obtained catalysts in 3.98 mL of MiliQ water, 1 mL of isopropanol and 20 μL of Nafion 5% wt, ultrasonicating for 15 min. The Pt loading of the different catalysts tested on the glassy carbon disk were about 7 $\mu g/cm^2_{disk}$. Cyclic voltammetry was performed at

room temperature in a N_2/Ar saturated 0.1 M $HClO_4$ solution at the sweep rate of 50 mV/s. The electrochemical active surface area (EASA) was determined by integrating the charge involved in the so-called hydrogen UPD region, assuming 210 $\mu C/cm^2$ for the total charge after the subtraction of the double layer contribution. Oxygen reduction reaction (ORR) measurements were conducted in O_2-saturated 0.1 M $HClO_4$ solutions by sweeping the potential from 0.05 to 1.05 V at the scan rate of 10 mV/s and a rotation speed of 1600 rpm. ORR polarization curves were normalized to the substrate's area (0.196 cm^2). The kinetic currents i_k at 0.9 V were calculated from the ORR polarization curves by considering the Koutecky-Levich equation:

$$\frac{1}{i} = \frac{1}{i_k} + \frac{1}{i_d} \rightarrow i_k = \frac{i_d \cdot i}{i_d - i}$$

where i is the current measured at 0.9 V, i_k is the kinetic current and i_d is the diffusion-limiting current. The electrode potential was controlled using a SP200 Biologic potentiostat.

Accelerated stability test were performed between 0.5 and 1.0 V at 50 mV/s for 4,000 cycles in N_2-saturated 0.1 M $HClO_4$. ORR polarization curves were obtained afterwards in O_2-saturated 0.1 M $HClO_4$ solutions, following the procedure described above.

Tables and figures

Inital Amount / mmol			Atomic Composition
$Pt(acac)_2$	$Ni(acac)_2$	$Co(acac)_2$	
0.2	0.5	0.0	$Pt_{44}Ni_{56}$
0.2	0.0	0.5	$Pt_{49}Co_{51}$
0.2	0.5	0.1	$Pt_{49}Ni_{49}Co_2$
0.2	0.5	0.5	$Pt_{36}Ni_{58}Co_6$
0.2	0.5	1.0	$Pt_{33}Ni_{52}Co_{15}$
0.2	0.5	3.0	$Pt_{31}Ni_{51}Co_{18}$
0.2	0.5	5.0	$Pt_{30}Ni_{51}Co_{19}$

Table S1. Initial amount of metal precursors and final atomic composition, measured by ICP-MS, of the PtNi, PtCo and PtNiCo nanoparticles synthesized at 130 ºC.

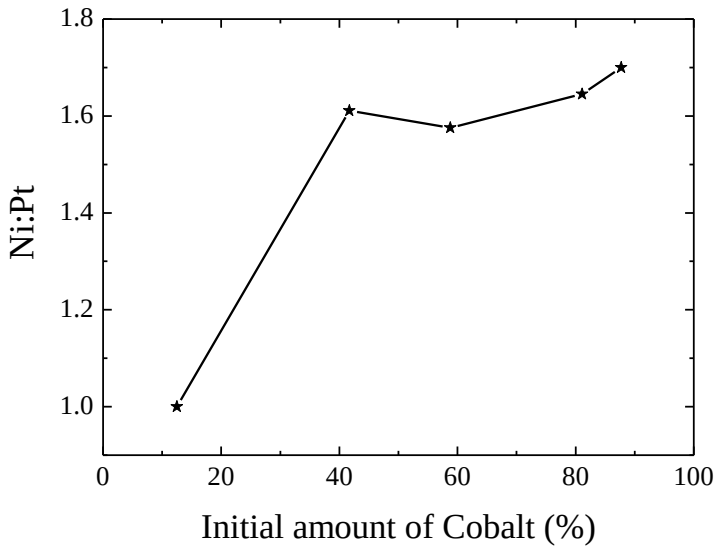

Figure S1. Ni:Pt ratio as function of the initial amount of cobalt precursor, of the PtNiCo nanoparticles synthesized at 130 ºC.

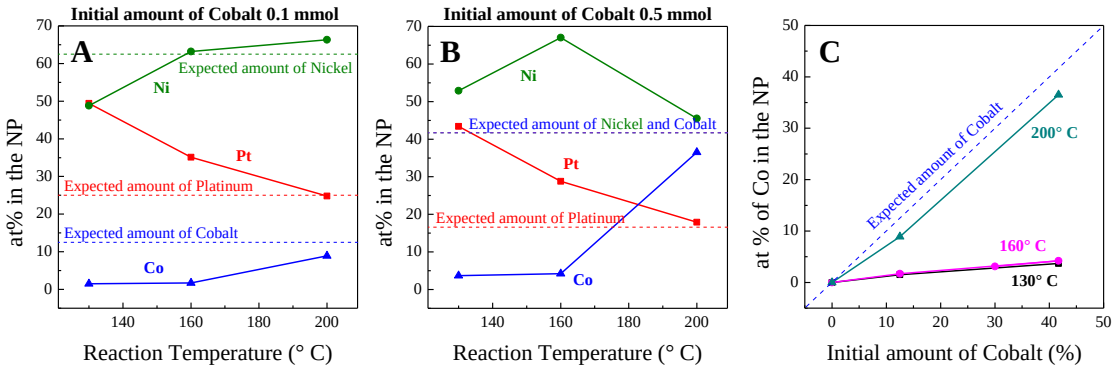

Figure S2. Reduction trend of three metals (Pt, Ni and Co) as a function of heating temperature. (A, B) Atomic composition of the trimetallic nanoparticles for a initial amount of Co precursor of 0.1 mmol and 0.5 mmol, respectively. (C) Atomic percentage of Co of the PtNiCo nanoparticles synthesized at different temperatures as a function of the initial amount of Co precursor. Dashed lines correspond to the expected composition if the entire precursor is reduced.

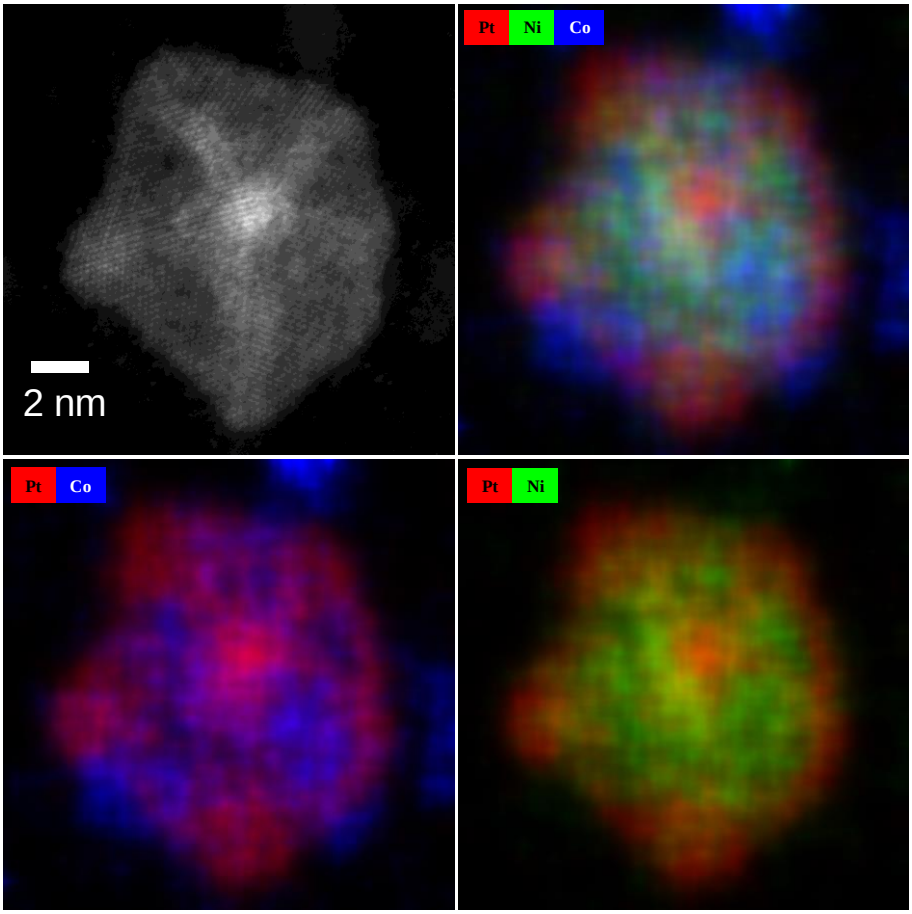

Figure S3. HAADF-STEM image of a PtNiCo decahedron obtained in the one-step synthesis showing a vertex where five facets are meeting (upper-left) and EDX elemental mapping of this nanoparticle. EDX showed $Pt_{37}Ni_{39}Co_{24}$ composition.

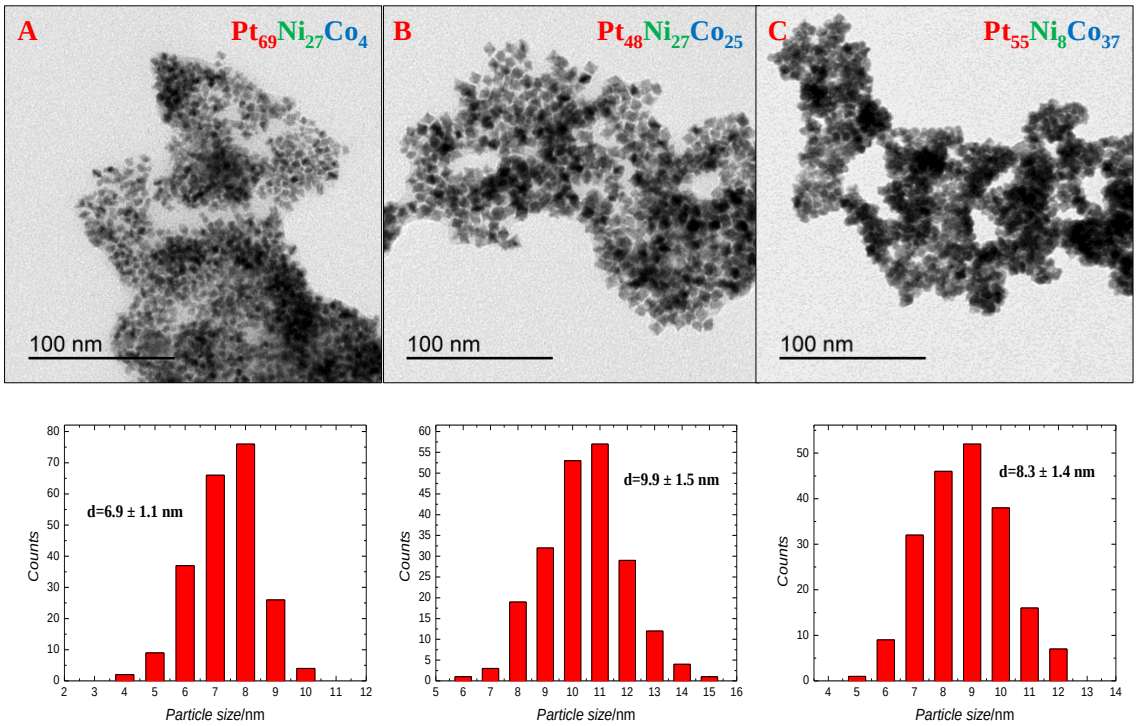

Figure S4. TEM images and particle size distribution of the PtNiCo nanoparticles obtained in the two-steps synthesis for the optimization of t_1 and t_2. (A) 16 h/26 h (B) 24 h/18 h (C) 32 h/10 h. The composition of the different samples was determined by ICP-MS. In the determination of the particle size distribution, octahedral and non-octahedral nanoparticles were taken into account.

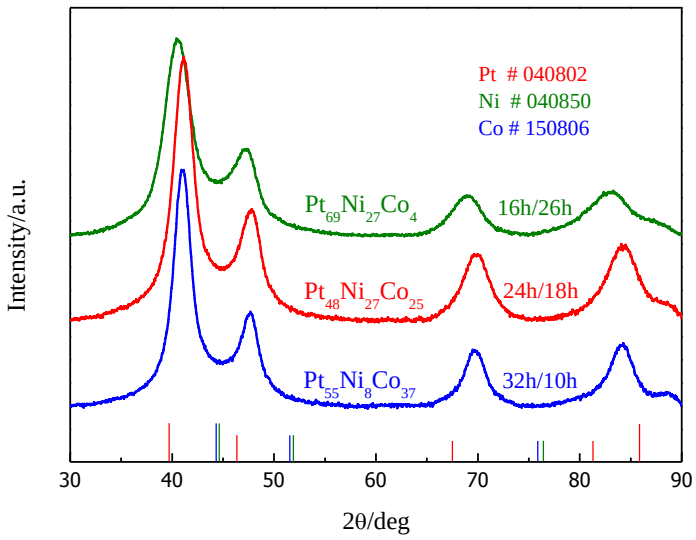

Figure S5. XRD patterns of PtNiCo nanoparticles obtained in the two-steps synthesis for the optimization of t_1 and t_2. Reaction temperature: 130 ºC.

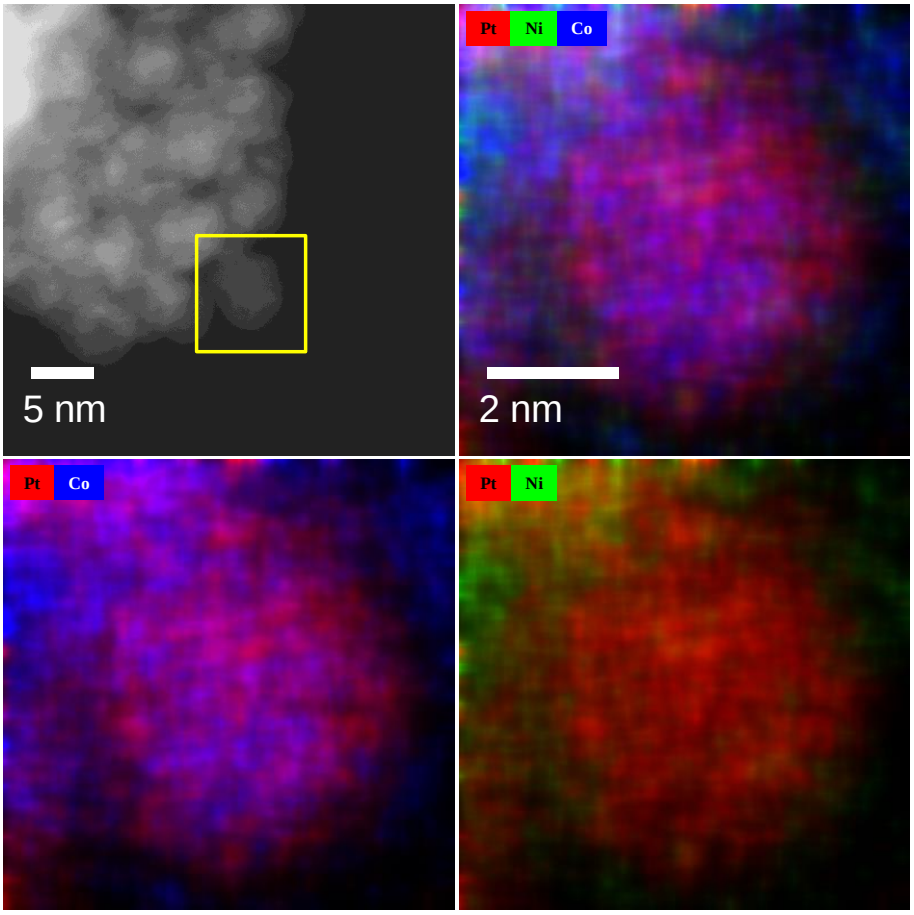

Figure S6. HAADF-STEM image and EDX elemental mapping of PtCo-rich nanoparticles found in the microscopic analysis of the PtNiCo electrocatalyst synthesized by the "two-step" synthetic route. EDX composition: $Pt_{55}Ni_9Co_{36}$.

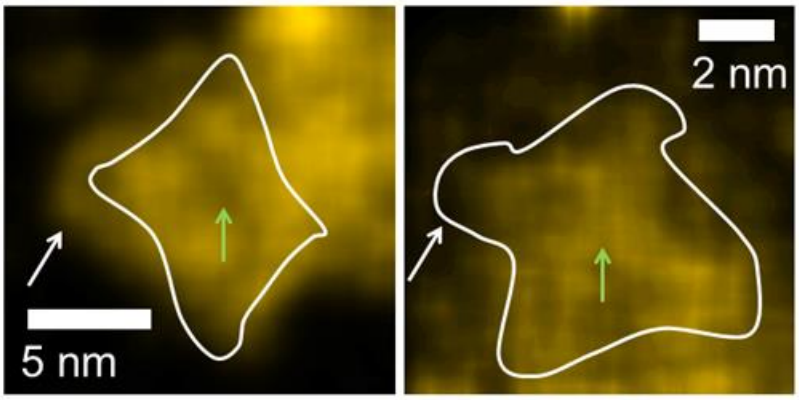

Figure S7. Co distribution in EDX elemental maps of PtNiCo nanoparticles synthesized by the "one-step" (left picture) and "two-step" (right picture) synthetic route. White lines signify the shape of the octahedra from HAADF images. White arrows highlight the Co distribution at the outer parts and green arrows highlight the Co distribution at the center parts of the octahedra.

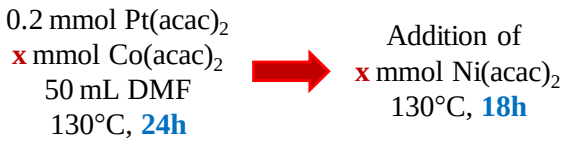

x	Atomic composition	Type
0.25 mmol + 0.25 mmol K(acac)	$Pt_{61}Ni_{26}Co_{13}$	$Pt_{1.5}M$
0.5 mmol	$Pt_{48}Ni_{27}Co_{25}$	PtM
0.75 mmol	$Pt_{38}Ni_{39}Co_{23}$	$PtM_{1.5}$

Table S2. Scheme of the "two-step synthesis" (24 h/18 h) for the control of the composition. The table resumes the amounts of metal precursors used in each synthesis, the atomic composition determined by ICP-MS and the type of nanoparticles obtained.

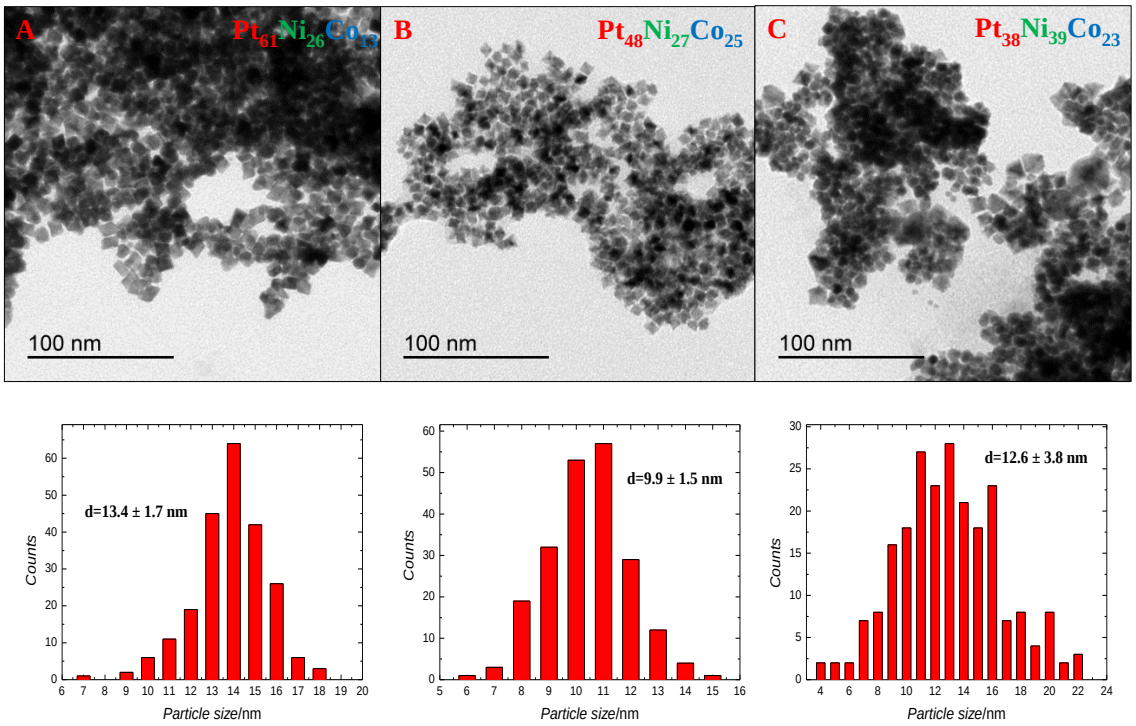

Figure S8. TEM images and particle size distribution of the PtNiCo nanoparticles obtained in the "two-step" synthesis (24 h/18 h). (A) Pt-rich (B) $Pt_{50}(NiCo)_{50}$ (C) Non-noble-rich nanocrystals. Reaction temperature: 130 ºC. The composition of the different samples was determined by ICP-MS. In the determination of the particle size distribution, octahedral and non-octahedral nanoparticles were taken into account.

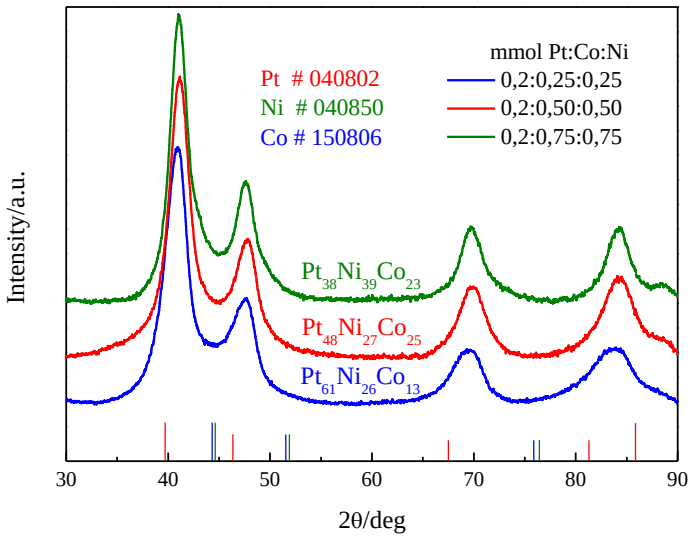

Figure S9. XRD patterns of PtNiCo nanoparticles obtained in the two-steps synthesis (24 h/18 h) for control of the composition. Reaction temperature: 130 ºC.

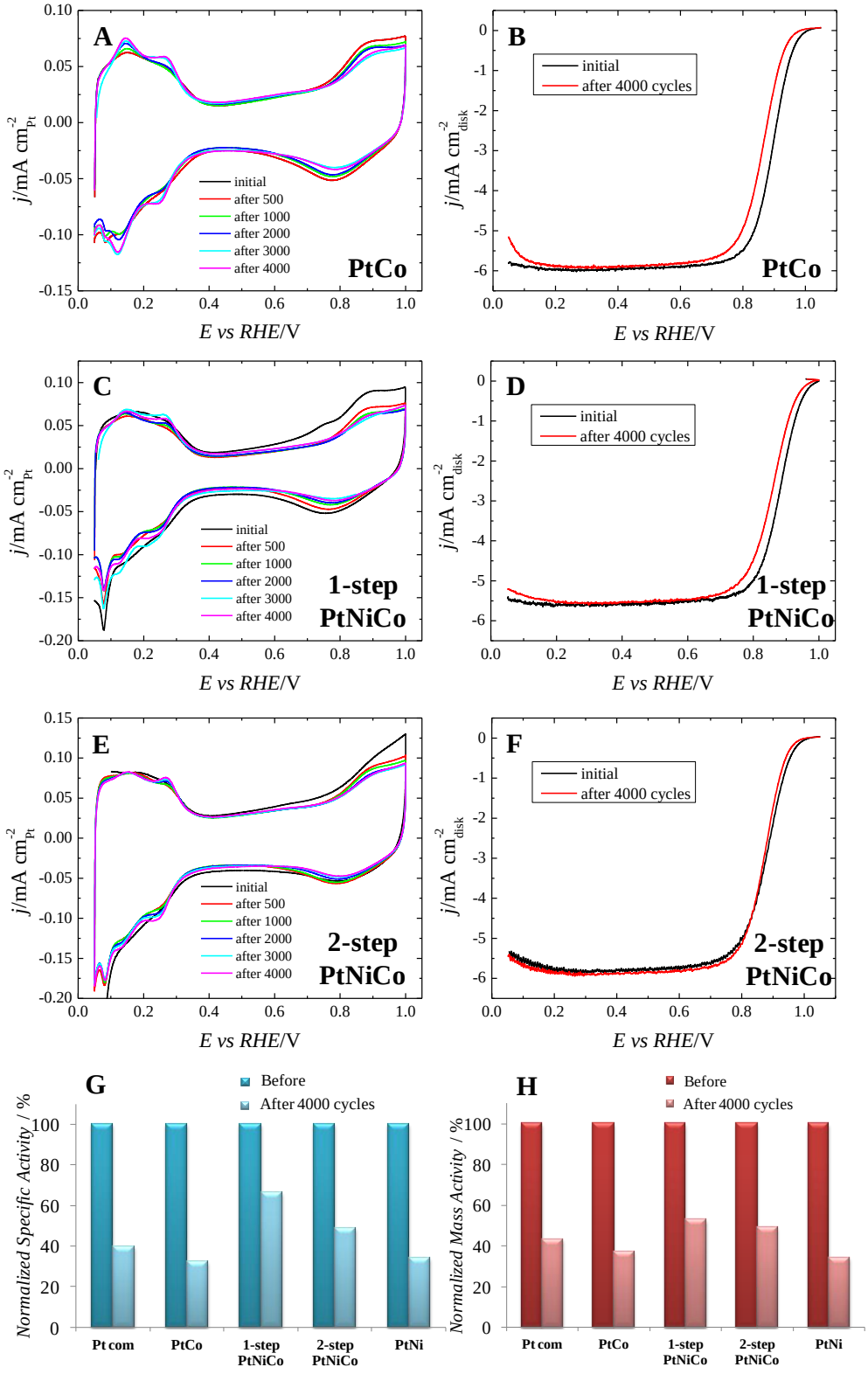

Figure S10. Specific and mass activities before and after stability test. CVs and ORR polarization curves, respectively, for PtCo/C (A, B), 1-step PtNiCo (C, D) and 2-step PtNiCo (E, F). Normalized specific and mass activities for commercial Pt/C and octahedral PtCo/C, 1-step PtNiCo/C, 2-step PtNiCo/C and PtNi/C nanocatalysts (G, H).

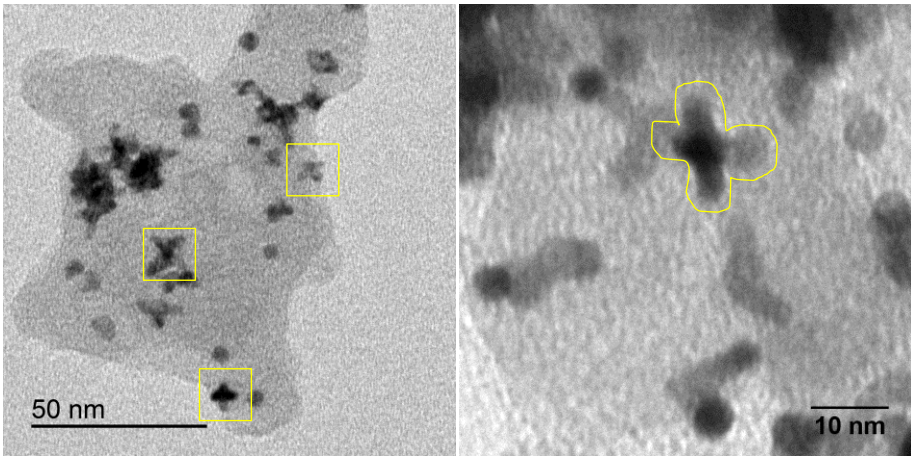

Figure S11. TEM images of "one-step" PtNiCo nanoparticles after 2000 potential cycles, showing the selective leaching in the facets and resulting in the formation of a skeleton type structure.

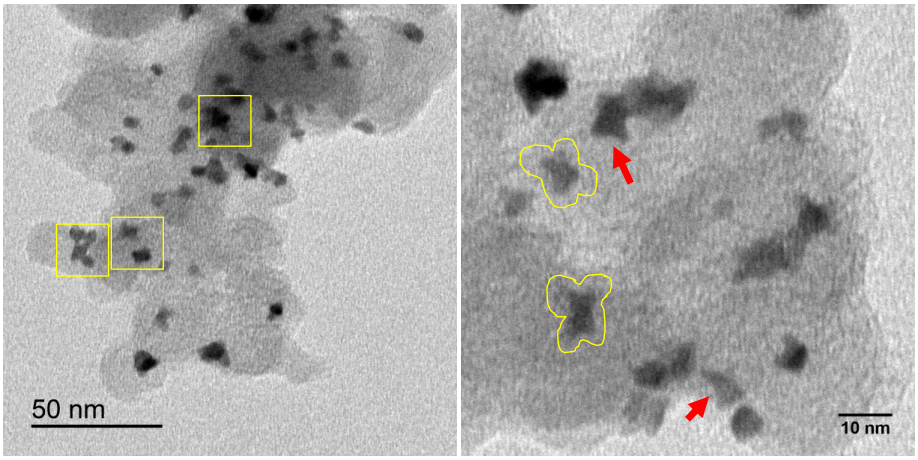

Figure S12. TEM images of "two-step" PtNiCo nanoparticles after 2000 potential cycles, showing the selective leaching in the facets and resulting in the formation of a skeleton type structure. Arrows point out nanooctahedra partially leached.

Supporting References

(1) Momma, K.; Izumi, F. *J. Appl. Crystallogr.* **2011**, *44*, 1272.